Diagnosis of soft faults in analog integrated circuits based on fractional correlation*

Deng Yong(邓勇)[1,2,†], Shi Yibing(师奕兵)[1], and Zhang Wei(张伟)[1]

[1]School of Automation Engineering, University of Electronic Science and Technology of China, Chengdu 611731, China
[2]School of Electronics and Information Engineering, Southwest Petroleum University, Chengdu 610500, China

Abstract: Aiming at the problem of diagnosing soft faults in analog integrated circuits, an approach based on fractional correlation is proposed. First, the Volterra series of the circuit under test (CUT) decomposed by the fractional wavelet packet are used to calculate the fractional correlation functions. Then, the calculated fractional correlation functions are used to form the fault signatures of the CUT. By comparing the fault signatures, the different soft faulty conditions of the CUT are identified and the faults are located. Simulations of benchmark circuits illustrate the proposed method and validate its effectiveness in diagnosing soft faults in analog integrated circuits.

Key words: analog circuits; soft faults; fault diagnosis; Volterra series; fractional correlation
DOI: 10.1088/1674-4926/33/8/085007 **EEACC:** 2570

1. Introduction

Fault diagnosis of analog components in mixed-signal circuits is receiving more and more attention. It is reported that 80% of the faults occur in the analog segments in the circuits[1]. Due to the lack of explicit fault models, the tolerance of analog components and circuit nonlinearities, fault diagnosis of analog components develops very slowly.

There are two kinds of faults in analog circuits—hard faults and soft faults[2,3]. The difference between these two faults is whether the topology of the CUT changes or the parameters of the analog parts vary greatly. Since soft faults are deviations of analog parts that result in the CUT's performance out of acceptable limits, and the deviations compared with the nominal parameters are not very clear as hard faults, it is more difficult to diagnose soft faults compared with hard faults. In recent years, there has been much research on analog fault diagnosis. The neural network method is widely used to identify fault models[4,5], and this is currently a popular technique to diagnose hard and soft faults in analog circuits. Fuzzy analysis is used to diagnose soft faults in linear analog circuits[6]. With the aim of solving the problems of soft fault diagnosis and tolerance in analog circuits, the method of the slope fault model combined with a test-point selection algorithm is proposed[7]. Based on defect-oriented testing[8], wavelet preprocessing is proposed to diagnose the faults of analog integrated circuits[9]. Both the methods of genetic algorithm (GA) and support vector machine (SVM) have been improved to be effective in extracting the soft fault signature[10,11]. Reference [12] used the particle swarm optimization (PSO) method to train SVM to improve the capability of fault diagnosis. Other methods such as analysis of the supply current[13], transfer functions[14], parameter sensitivity[15] and linear relativity of the node-voltage increments[16] are also proposed to solve the problem of soft fault diagnosis in analog circuits.

However, the aforementioned diagnosis methods are not good at locating the fault after completing soft fault detection. To solve this problem, Reference [17] uses the coherence function to extend the scheme in Ref. [9] and improve the soft fault diagnosis capability, especially in locating the faulty components. However, Reference [17] neglects the influence of nonlinearity in analog circuits. In practical applications, faulty analog circuits commonly exhibit certain weak nonlinearities that cannot be sufficiently estimated by conventional linear models, even if the fault-free case of the circuit can be analyzed by the linear method.

To solve the problem of nonlinearity, the adaptive subband Volterra filter (AVF)[18] is used, which is a kind of Volterra model. But the soft fault features are too small to identify, the Volterra model in Ref. [18] should be improved further.

This paper proposes a new technique of soft fault diagnosis that is suitable for both linear components and weak nonlinear components in analog circuits. It is based on the Volterra series and the fractional correlation to extract the fault signatures. The proposed method is made adaptive to the influence of weak nonlinearity.

2. Diagnosis principles

2.1. Fault models

To find the relations between the output and input signals, the Volterra series are introduced first. A class of nonlinear systems can be characterized by the Volterra series, and these systems have cause, stability and time-invariability features[19]. The Volterra series reflects the fundamental features of the system and will not change unless faults occur. The Volterra series of a nonlinear system is given by Eq. (1)[20,21].

* Project supported by the Program for New Century Excellent Talents in University, China (No. NCET-05-0804) and the Chinese National Programs for High Technology Research and Development (No. 2006AA06Z222).
† Corresponding author. Email: y_den117@126.com
Received 25 August 2011, revised manuscript received 28 October 2011

$$y(n) = y_1(n) + y_2(n) + \cdots + y_i(n) + e(n),$$
$$\begin{cases} y_1(n) = \sum_m h_1(m)u(n-m) \\ \cdots \\ y_i(n) = \sum_{m_1}\cdots\sum_{m_i} h_i(m_1,\cdots,m_i)\prod_{m_i} u(n-m_i), \end{cases} \quad (1)$$

where $h_i(m_1,\cdots,m_i)$ is the ith-order Volterra series, $u(n)$ is the input signal, $y(n)$ is the output signal and $y_i(n)$ is the ith-order output signal. $e(n)$ is the error between the ideal and estimated $y(n)$.

$y_i(n)$ can be identified from $y(n)$ by the Vander monde method[22]. Equation (1) is available for fault-free and faulty circuits. Different faults induce different $h_i(m_1,\ldots,m_i)$, but the dimensional disaster of the Volterra series makes the complexity of computation increase in a geometric series way[23]. For example, if $N_1 = N_2 = N_3 = 30$, the dimensions of the first-, second- and third-order Volterra series are 30, 465 and 4960, respectively. This shows that calculation of the Volterra series is difficult. If only two orders are used, then the complexity of the computation will be decreased, but in full-band domain the soft fault signatures cannot be extracted distinctly from the first- and second-order Volterra series because the fault signatures are insufficient. Considering this problem, a Volterra series based on fractional wavelet packet transform (FRWPT) is introduced, which is a fractional subband filtering technology.

2.2. FRWPT of the Volterra series

From Ref. [24], the fractional Fourier transform (FRFT) of a continuous-time function $f(t)$ is

$$f^\alpha(u) = \begin{cases} \int f(t)K_\alpha(u,t)\mathrm{d}t, & \alpha \neq l\pi, \\ f(t), & \alpha = 2l\pi, \\ f(-t), & \alpha = (2l\pm 1)\pi, \end{cases} \quad (2)$$

where α is the angle parameter and the kernel function of FRFT is

$$K_\alpha(u,t) = \sqrt{\frac{1-\mathrm{j}\cot\alpha}{2\pi}}\mathrm{e}^{\mathrm{j}[(u^2+t^2)\cot\alpha/2 - ut\csc\alpha]}. \quad (3)$$

The kernel function of FRFT can be replaced by that of FRWPT as

$$K_\alpha(p,n,i,k) = \sqrt{\frac{1-\mathrm{j}\cot\alpha}{2\pi}}\phi_{i,k}(n) \times \mathrm{e}^{\mathrm{j}[(p^2+n^2)\cot\alpha/2 - pn\csc\alpha]}, \quad \alpha \neq l\pi, \quad (4)$$

where

$$\phi_{i,k}(n) = \frac{1}{2^{i/2}}\phi\left(\frac{n}{2^i} - k\right), \quad (5)$$

and where $\phi(n)$ is the mother wavelet, i is the scale parameter and k is the shift parameter.

Therefore, $u(n)$ can be transformed as

$$\begin{cases} u^\alpha(p,i,k) = \sum_n u(n)K_\alpha(p,n,i,k), \\ u(n) = \sum_{p,i,k} u^\alpha(p,i,k)K_{-\alpha}(p,n,i,k), \end{cases} \quad (6)$$

and $y_1(n)$ can be transformed as

$$\begin{cases} y_1^\alpha(p',i',k') = \sum_n y_1(n)K_\alpha(p',n,i',k'), \\ y_1(n) = \sum_{p',i',k'} y_1^\alpha(p',i',k')K_{-\alpha}(p',n,i',k'). \end{cases} \quad (7)$$

In the fractional wavelet packet domain, the output of the first-order component is

$$y_1^\alpha(p',i',k') = \sum_n\sum_m\sum_{p,i,k}[u^\alpha(p,i,k)h_1^\alpha(m,i,k,i',k') \times \psi(p,p',n,m,\alpha)], \quad (8)$$

where

$$\psi(p,p',n,m,\alpha) = \mathrm{e}^{-\mathrm{j}\{[p^2+p'^2+(n-m)^2+n^2]\cot\alpha/2 - [p(n-m)-p'n]\csc\alpha\}}. \quad (9)$$

$y_1^\alpha(p',i',k')$ and $u^\alpha(p,i,k)$ can be calculated from the output and input signal $y(n)$ and $u(n)$ that are directly measured at the output and input node. According to the LMS (least mean square) method, the first-order fractional Volterra series, $h_1^\alpha(m,i,k,i',k')$, can be obtained.

$y_2(n)$ can be transformed as

$$\begin{cases} y_2^\alpha(p',i',k') = \sum_n y_2(n)K_\alpha(p',n,i',k'), \\ y_2(n) = \sum_{p',i',k'} y_2^\alpha(p',i',k')K_{-\alpha}(p',n,i',k'). \end{cases} \quad (10)$$

In the fractional wavelet packet domain, the output of the second-order component is

$$y_2^\alpha(p',i',k') = \sum_n\sum_{m_1,m_2}\sum_{\substack{p_1,p_2\\ i_1,k_1\\ i_2,k_2}}[u^\alpha(m,i_1,k_1)u^\alpha(m,i_2,k_2) \times h_2^\alpha(m_1,m_2,i_1,k_1,i_2,k_2,i',k') \times \varphi(p_1,p_2,p',n,m_1,m_2,\alpha)], \quad (11)$$

where

$$\varphi(p_1,p_2,p',n,m_1,m_2,\alpha) = \exp\left(-\mathrm{j}\left\{\left[p_1^2+p_2^2-p'^2+(n-m_1)^2+(n-m_2)^2-n^2\right] \times\cot\alpha/2 - [p_1(n-m_1)+p_2(n-m_2)-p'n]\csc\alpha\right\}\right). \quad (12)$$

The second-order fractional Volterra series, $h_2^\alpha(m_1,m_2,i_1,k_1,i_2,k_2,i',k')$, can be obtained the same way as the first-order fractional Volterra series.

2.3. Extracting the fault signatures

After the first and second-order fractional Volterra series are calculated from the CUT, the fractional correlation functions can be calculated to diagnose the soft fault. The cross fractional correlation function[25] between two continuous-time functions $f_1(t)$ and $f_2(t)$ is

$$(f_1 \otimes_\alpha f_2)(\rho) = \int f_1^\alpha(\upsilon)[f_2^\alpha(\upsilon-\rho)]^*\mathrm{d}\upsilon, \quad (13)$$

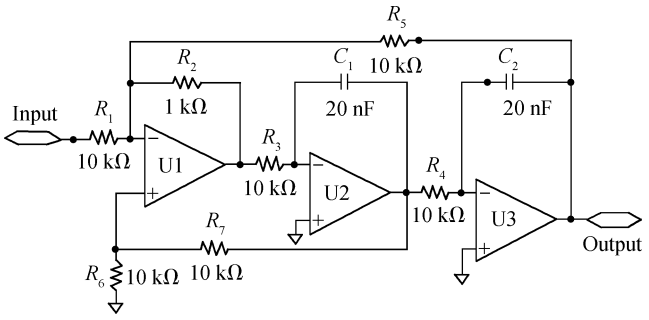

Fig. 1. The state variable filter circuit in simulation 1.

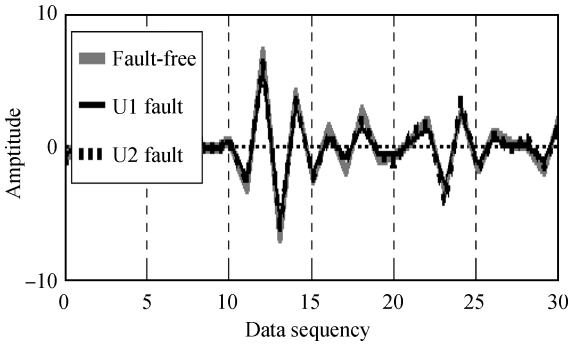

Fig. 2. First-order fractional Volterra series when $\alpha = \pi/2$.

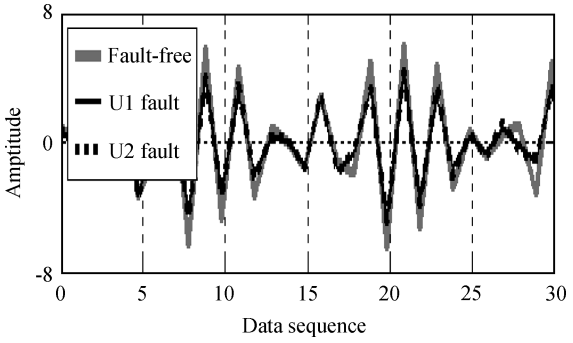

Fig. 3. Second-order fractional Volterra series when $\alpha = \pi/2$.

where * denotes the conjugate function.

In the discrete domain, Equation (13) is

$$(f_1 \otimes_\alpha f_2)(u) = \sum_l f_1^\alpha(l)[f_2^\alpha(l-u)]^*. \tag{14}$$

Hence the cross fractional correlation function of the first- and second-order fractional Volterra series sequence of the CUT is

$$\begin{cases} (h_1 \otimes_\alpha \overline{h}_1)(u) = \sum\limits_l h_1^\alpha(l)[\overline{h}_1^\alpha(l-u)]^*, \\ (h_2 \otimes_\alpha \overline{h}_2)(u) = \sum\limits_{l_1,l_2} h_2^\alpha(l_1,l_2)[\overline{h}_2^\alpha(l_1-u,l_2-u)]^*, \end{cases} \tag{15}$$

where $h_1^\alpha(l)$ and $h_2^\alpha(l_1,l_2)$ are the simplified forms of $h_1^\alpha(m,i,k,i',k')$ and $h_2^\alpha(m_1,m_2,i_1,k_1,i_2,k_2,i',k')$; h and $\overline{h}$ denote the Volterra series sequence of the fault-free case and the faulty case of the CUT, respectively.

Based on Eq. (15), two fault signature variables can be constructed as

$$\begin{cases} V_1(\alpha_1) = \int \left|(h_1 \otimes_\alpha \overline{h}_1)(u)\right| \mathrm{d}u \Big/ \int \left|(h_1 \otimes_\alpha h_1)(u)\right| \mathrm{d}u, \\ V_2(\alpha_2) = \int \left|(h_2 \otimes_\alpha \overline{h}_2)(u)\right| \mathrm{d}u \Big/ \int \left|(h_2 \otimes_\alpha h_2)(u)\right| \mathrm{d}u. \end{cases} \tag{16}$$

The cross fractional correlation function of the Volterra series sequences represents the fundamental differences of two circuits or two conditions of the one circuit. Different faults will induce different V_1 and V_2. Therefore, the two variables can be used as the fault features.

3. Simulation

In this section, simulations will be carried on to illustrate the idea of the paper. The Haar wavelet is selected as the mother wavelet and the pyramid architect is used. All the simulation work is finished on a PC with 3.0 GHz, 1 GB.

3.1. Simulation 1

In this part the benchmark circuit, the state variable filter as shown in Fig. 1, is studied[9, 17]. The parameters of all the components are labeled in the figure.

If the CUT is fault-free, it will show the feature of linearity. However, if the operational amplitude (OA) is faulty, the CUT will exhibit the nonlinearity of the CUT[9]. Based on the Volterra series that is available for both nonlinear and linear circuits (only the first-order Volterra series is used), the proposed method studies the soft faults and the nonlinearity coming from the OA fault.

Table 1. The fault set of simulation 1.

Fault No.	Fault type	Fault value
1	Fault-free	
2	R1 5% fault	10–10.5 kΩ
3	R2 10% fault	1–1.1 kΩ
4	R5 –8% fault	10–9.2 kΩ
5	C1 6% fault	20–21.2 nF
6	C2 –10% fault	20–18 nF
7	U1 12% fault	0%–12%
8	U2 9% fault	0%–9%

The linear circuits are considered as a kind of specialty nonlinear circuit. The tolerance of resistances is $0 \pm 5\%$ of its nominal value, the tolerances of other components are $0 \pm 6\%$ of their nominal values, and the stimulus signal is a 1 kHz sinusoidal signal[17].

Apart from the R_1 and C_1 faulty cases studied in Ref. [17], the fault-free case and the five randomly selected soft faulty cases will be studied, and are shown in Table 1. In the seven faulty cases, there are two faulty OA cases, which assumes that the OA transistor is soft faulty in nonlinearity.

The simulation is done using HSPICE at first, and the sampled signals are processed by the fractional correlation program written by the authors. Cases of U1 and U2 faults are used to explain the steps of extracting the fault signatures. Figures 2–7 show the fault diagnosis effectiveness of the proposed method.

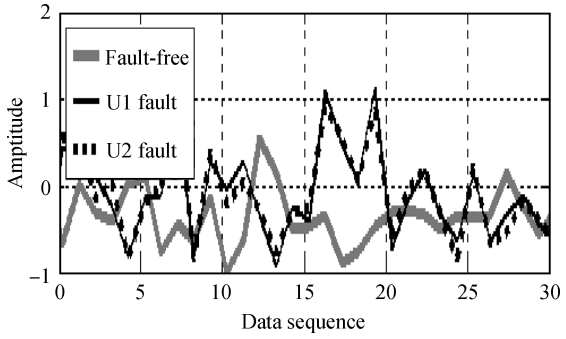

Fig. 4. First-order fractional Volterra series ($\alpha = 3\pi/10$).

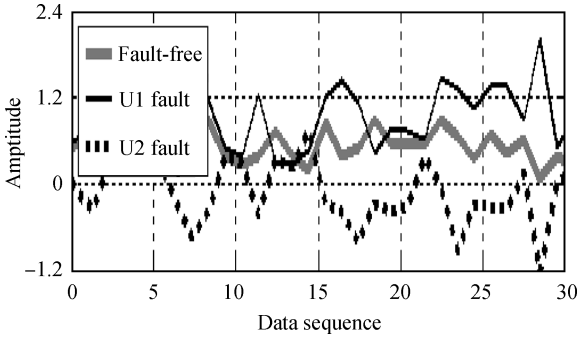

Fig. 5. Second-order fractional Volterra series ($\alpha = 3\pi/10$).

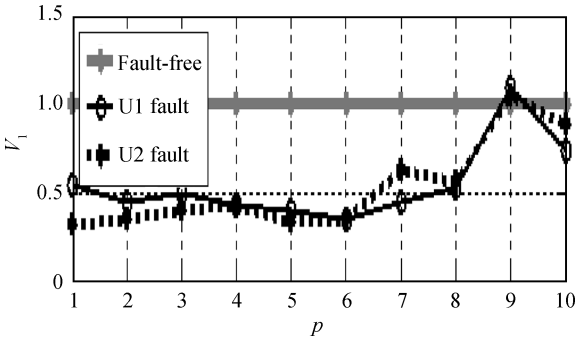

Fig. 6. V_1 in different α_1.

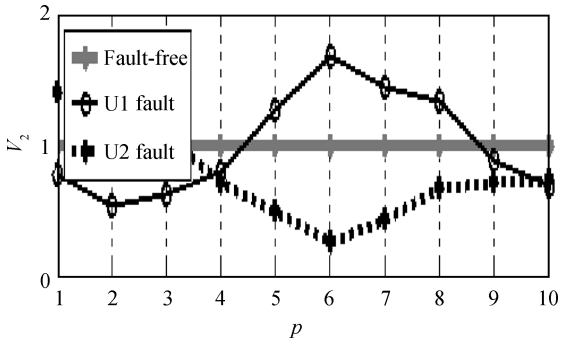

Fig. 7. V_1 in different α_2.

The representative frequency bands[17] of the wavelet filter for the signatures are decided by that in $\alpha = \pi/2$. The Volterra series waveform in $\alpha = \pi/2$ is shown in Figs. 2 and 3. In the simulation the representative frequency band is subband 5 by comparison.

In Fig. 3, there is a small difference among the three waveforms. Although the difference is too small to be fault signatures, it could be processed further. There is no difference in the waveforms in Fig. 2, which indicates that the linear method is not fit for diagnosing the nonlinear components. To extract the fault signatures V_1, V_2 in Eq. (16), α is set within the range of 0, $\pi/2$. The results of $\alpha = 3\pi/10$ in subband 5 are shown in Figs. 4 and 5.

Figures 4 and 5 give the waveforms when α is changed to $3\pi/10$. In Fig. 5, the difference in the three waveforms has been enlarged, which is enough to isolate the three cases. This shows that we can detect and locate the soft faulty components with weak nonlinearity by changing α. The fault signatures V_1 and V_2 in different α are shown in Figs. 6 and 7, where α is obtained by $p\pi/20$ ($p = 1, 2, \cdots, 10$).

From Figs. 6 and 7, we can find that when $\alpha = \pi/2$ (the Fourier transform is used), then the difference of the three cases is small. It could be noted that V_1 and V_2 of the fault-free case is equal to 1 constantly. By changing the α value, the differences in the three cases becomes clear, especially that of V_2. Since V_2 extracts the nonlinearity feature, the difference in V_2 of the three cases is clearer than that of V_1, which is shown in Figs. 6 and 7.

Table 2 gives the results of the fractional correlation for all eight cases, which can accurately show how the soft fault signatures are extracted. Due to the limitation of the length of the paper, only the results of $\alpha = 3\pi/10, 4\pi/10, 5\pi/10$ in subband 5 are listed. Take the instances of R_1 and C_1, V_1 of R_1 in $\alpha = \pi/2$ is 147% that of the fault-free case, while that of the C_1 fault case is 144.1%. V_2 of R_1 in $\alpha = \pi/2$ is 185.2% that of the fault-free case, while that of the C_1 fault case is 179.6%. It is difficult for us to isolate R_1 and C_1 faults even if we know that some fault has occurred. However, if $\alpha = 4\pi/10$, V_1 of R_1 is 241.3%, while that of the C_1 fault case is 192.2%. V_2 of R_1 is 78.1%, while that of the C_1 fault case is 44.9%. Thus the difference in the cases is given significantly.

Figures 2–5 can be explained by the results of Table 2. V_1 of U1 in $\alpha = \pi/2$ is 73.5 that of the fault-free case, while that of the U2 fault case is 87.3. V_2 of U1 in $\alpha = \pi/2$ is 69.5%, while that of the U2 fault case is 73.7%. If $\alpha = 3\pi/10$, V_1 of R_1 is 34%, while that of the U2 fault case is 34.6%. V_2 of U1 is 166.9%, while that of U2 is 25.6%.

To show the advantages of the proposed method, it is compared with another existing method in Table 3. For each CUT case, Monte-Carlo experiments are done. To analyze the real-time performance of the proposed method, the mean running time for each case is listed in Table 3. From Table 3 we can observe that the proposed method has a better recognition capability than that of the method in Ref. [18], which also uses the Volterra series to diagnosis analog circuits. The mean fault recognition rate of the proposed method is 97.5%, while its worst fault recognition rate is 92.5% (in the U1 fault), which are both better than the other method. This shows that the proposed method can diagnose all eight proposed cases of the CUT. The mean fault recognition rate of the method in Ref. [18] is 93.3%, which is good enough in practical fault diagnosis. However, it is not good at diagnosis of the U1 and U2 faults, and its worst fault recognition rate is 79.5% (in the U2

Table 2. Results of the diagnosis in simulation 1.

Fault No.	Fault type	V_1 of fractional correlation (%)			V_2 of fractional correlation (%)		
		$\alpha = 3\pi/10$	$\alpha = 4\pi/10$	$\alpha = 5\pi/10$	$\alpha = 3\pi/10$	$\alpha = 4\pi/10$	$\alpha = 5\pi/10$
1	Fault-free	100.0	100.0	100.0	100.0	100.0	100.0
2	R1 5% fault	193.0	241.3	147.0	76.5	78.1	185.2
3	R2 10% fault	158.7	121.9	75.9	44.1	138.0	136.3
4	R5 –8% fault	67.6	118.3	69.6	169.8	119.0	33.8
5	C1 6% fault	87.7	192.2	144.1	138.4	44.9	179.6
6	C2 –10% fault	131.9	32.0	33.7	89.2	28.6	49.6
7	U1 12% fault	34.0	52.6	73.5	166.9	132.0	69.5
8	U2 9% fault	34.6	55.8	87.3	25.6	66.3	73.7

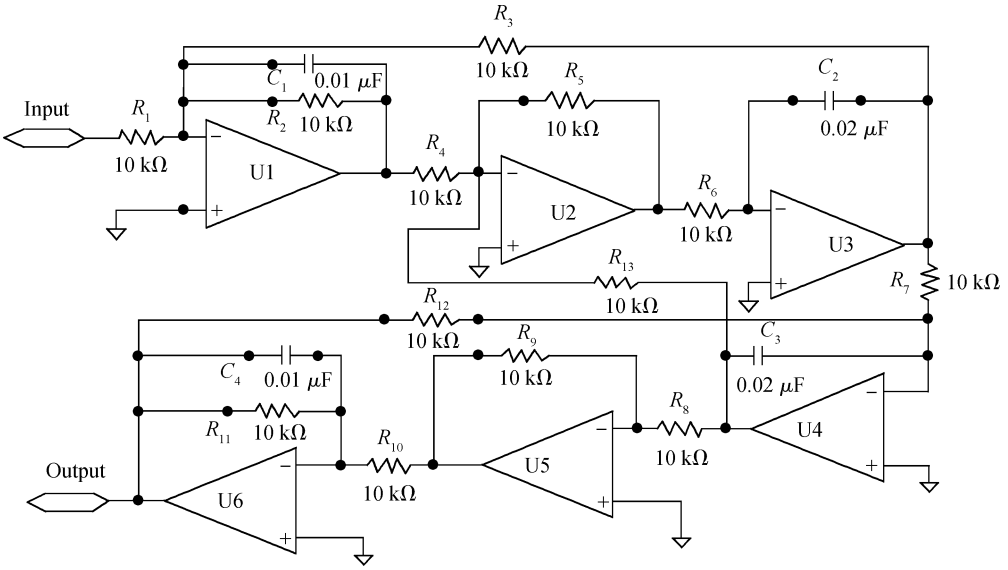

Fig. 8. The leapfrog filter circuit for simulation 2.

Table 3. Fault recognition rates (%) and running times (s) in simulation 1.

Fault No.	Fault type	Proposed method		Method of Ref. [18]	
		Fault recognition rate	Running time	Fault recognition rate	Running time
1	Fault-free	100	8.8	100	10.3
2	R1 5% fault	99	9.1	98.0	10.1
3	R2 10% fault	97	9.1	96.5	10.1
4	R5 –8% fault	99	9	99	10.2
5	C1 6% fault	98.5	8.7	95.5	10.2
6	C2 –10% fault	100	8.6	96	10.1
7	U1 12% fault	92.5	8.7	82.0	10.4
8	U2 9% fault	94	8.8	79.5	10.4
Mean recognition rate		97.5		93.3	
Mean running time			8.9		10.2

fault), less than that of the proposed method. The reason that the fault recognition rates of some cases are less than 100% is the aliasing of the faults. To avoid the problem, α in the proposed method can use smaller steps. However, it will improve the complexity of computation and decrease the real-time performance. There are no significant differences in the real-time performance between the two methods according to the running times, which shows that the proposed method doesn't improve the real-time fault diagnosis capability.

3.2. Simulation 2

To show the universality of the proposed method, the leapfrog filter circuit[9,17] is considered in Fig. 8. The nominal parameters for all components are labeled in the figure. The stimulus signal and tolerances are the same as simulation 1.

For comparison, the fault-free case and seven soft fault cases are considered in Table 4. The fault cases are analyzed by the proposed method in the same way as simulation 1. For each CUT case, Monte-Carlo experiments are done. The diagnosis results and the running times used to analyze the real-time performance are shown in the table.

From Table 4 we can draw the conclusion that the proposed method outperforms the method in Ref. [18] when diagnosing weak nonlinear soft faults such as fault Nos. 6 and 7. This is an-

Table 4. Fault recognition rates (%) and running times (s) in simulation 2.

Fault No.	Fault type	Proposed method		Method of Ref. [18]	
		Fault recognition rate	Running time	Fault recognition rate	Running time
1	Fault-free	100	14.3	100.0	15.9
2	R1 5% fault	98.5	14.1	96.0	15.9
3	R8 7% fault	100	14.2	100.0	15.8
4	C1 11% fault	97	14.5	96.5	15.8
5	C3 –10% fault	100	14.4	97.0	15.8
6	U1 6% fault	96	14.4	80.0	15.9
7	U4 –12% fault	94.5	14.2	78.5	15.9
8	(R7&R9) 5% fault	100	14.3	95.0	16.0
Mean recognition rate		98.3		92.9	
Mean running time			14.3		15.9

other example to show the advantages of the proposed method. As for the real-time performance, the two methods are similar.

4. Conclusion

To solve the problem of diagnosing soft faults in analog circuits, a novel method is proposed in this paper. In the method, we derive an explicit fractional correlation model and construct soft fault signatures. Simulation results show that this method can extract the fault signatures of analog circuits properly. The proposed method makes a significant improvement to the method used in Ref. [18] and can be used in the soft fault diagnosis of linear and weak nonlinear components, which is very helpful.

References

[1] Li F, Woo P Y. Fault detection for linear analog IC-the method of short-circuits admittance parameters. IEEE Trans Circuits Syst I, 2002, 49(1): 105

[2] Sunil R D, Jila Z, Satyendra B, et al. Testing analog and mixed signal circuits with built in hardware: a new approach. IEEE Trans Instrum Meas, 2007, 56(3): 840

[3] Kodagunturi R, Bradley E, Maggard K, et al. Benchmark circuits for analog and mixed-signal testing. Southeastcon Proc of IEEE Kentuchy, 1999: 217

[4] Mohsen A A K, El-Yazeed M F A. Selection of input stimulus for fault diagnosis of analog circuits using ARMA model. Int J Electron Commun, 2004, 58(3): 212

[5] Aminian F, Aminian M, Collins H W. Analog fault diagnosis of actual circuits using neural networks. IEEE Trans Instrum Meas, 2002, 51(3): 544

[6] Wang P, Yang S Y. A new diagnosis approach for handling tolerance in analog and mixed-signal circuits by using fuzzy math. IEEE Trans Circuits Syst I, 2005, 52(10): 2118

[7] Yang C L, Tian S L, Long B, et al. Methods of handling the tolerance and test-point selection problem for analog-circuit fault diagnosis. IEEE Trans Instrum Meas, 2011, 60(1): 176

[8] Milor L, Visvanathan V. Detection of catastrophic faults in analog integrated circuits. IEEE Trans Computer-Aided Design, 1989, 8(2): 114

[9] Roh J, Abraham J A. Subband filtering for time and frequency analysis of mixed-signal circuit testing. IEEE Trans Instrum Meas, 2004, 53(2): 602

[10] Mao Y, Zhou X B , Pi D Y, et al. Parameters selection in gene selection using Gaussian kernel support vector machine by genetic algorithm. Journal of Zhejiang University Science, 2005, 6(10): 961

[11] Wang A, Li Y L, Zhao F Y, et al. Novel semi-supervised classification algorithm based on TSVM. Chinese Journal of Scientific Instrument, 2011, 32 (7): 1546

[12] Tu C J , Chuang L Y, Chang J Y, et al. Feature selection using PSO-SVM. Int J Computer Science, 2007, 33(1): 111

[13] Swarup B, Arijit R, Kaushik R. Frequency specification testing of analog filters using wavelet transform of dynamic supply current. Journal of Electronic Testing: Theory and Applications, 2005, 21: 243

[14] Zhen G, Jacob S. Coefficient-based test of parametric faults in analog circuits. IEEE Trans Instrum Meas, 2006, 55(1): 150

[15] Li Y J, Chen S J, Wang H J, et al. Application of voltage sensitivity vector in analog circuit fault diagnosis. Journal of Electronic Measurement and Instrument, 2009, 23(6): 29

[16] Hu G, Wang H, Yang S Y. A fault diagnosis method for non-linear analog circuits. Journal of Computer-Aided Design & Computer Graphics, 2009, 21(1): 1

[17] Xie Y L, Li X F. A method to locate parametric faults in analog integrated circuits. Journal of Semiconductors, 2008, 29(3): 598

[18] Trevor G B, Rafik A G, Franck B. Nonlinear system identification using a subband adaptive Volterra filter. IEEE Trans Instrum Meas, 2009, 58(5):1389

[19] Evans C, Rees D, Jones L, et al. Periodic signals for measuring nonlinear Volterra kernels. IEEE Trans Instrum Meas, 1996, 45(2): 362

[20] Avargel Y, Cohen I. Modeling and identification of nonlinear systems in the short-time Fourier transform domain. IEEE Trans Signal Process, 2010, 58(1): 291

[21] Rugh W J. Nonlinear system theory-the Volterra/Wiener approach. The Johns Hopkins University Press, 1981

[22] Chua L O, Liao Y L. Measuring Volterra Kernels II. Int J Circuit Theory and Applications, 1988, 17: 151

[23] Ou W, Han C Z, Wang W Z. Application of Volterra series in the identification of nonlinear systems. Control and Decision, 2002, 17(2): 239

[24] Almeida L B. The fractional Fourier transform and time-frequency representations. IEEE Trans Signal Process, 1994, 42(11): 3084

[25] Akay O, Boudreaux-Bartels G F. Fractional convolution and correlation via operator methods and an application to detection of linear FM signals. IEEE Trans Signal Process, 2001, 49(5): 979